Scientific Research Publishing

Open Journal of Applied Sciences, 2026, 16(11), 4304-4318
https://www.scirp.org/journal/ojapps
ISSN Online: 2165-3925
ISSN Print: 2165-3917

Response Surface Optimization of a Cocoa Husk-Based Biosorbent for the Removal of Phosphate Ions

Christian Landry Yapi[1], Yapo Hermann Aristide Yapi[1], David Léonce Kouadio[1], Kouassi Serge Gbamélé[2], Issifou Ouattara Mama[1], Brou Dibi[1]

[1]Laboratory of Environmental Sciences and Technologies, Jean Lorougnon Guédé University, Daloa, Côte d'Ivoire
[2]Laboratory of Environmental Sciences, Training and Research Unit (UFR) of Environmental Sciences and Management, Nangui Abrogoua University, Abidjan, Côte d'Ivoire
Email: zindrolandry@gmail.com

How to cite this paper: Yapi, C.L., Yapi, Y.H.A., Kouadio, D.L., Gbamélé, K.S., Mama, I.O. and Dibi, B. (2026) Response Surface Optimization of a Cocoa Husk-Based Biosorbent for the Removal of Phosphate Ions. *Open Journal of Applied Sciences*, **16**, 4304-4318.
https://doi.org/10.4236/ojapps.2026.1611234

Received: August 7, 2026
Accepted: November 7, 2026
Published: November 10, 2026

Copyright © 2026 by author(s) and Scientific Research Publishing Inc.
This work is licensed under the Creative Commons Attribution International License (CC BY 4.0).
http://creativecommons.org/licenses/by/4.0/

Open Access

Abstract

Eutrophication of surface waters, driven by excessive phosphorus discharges, constitutes a major threat to aquatic ecosystems. The objective of this work was to identify the best conditions for preparing a cocoa husk biosorbent intended for phosphate removal, using a design-of-experiments approach. After the key factors had been selected with a Plackett-Burman screening matrix, a two-level factorial design was carried out. Although globally significant ($p = 0.021$), the resulting linear model proved inadequate (adjusted $R^2 = 63.88\%$), justifying recourse to a central composite design. The resulting quadratic model exhibited excellent statistical performance ($R^2 = 97.16\%$; adjusted $R^2 = 95.13\%$; coefficient of variation = 0.72%), confirming its predictive robustness. Optimization via the desirability function identified a NaOH concentration of 1 N and an activation time of 8 hours as the optimal conditions. During validation tests, a mean removal rate of 98.23% was obtained, in agreement with the predicted value of 99.67%. These results confirm the efficiency of the biosorbent and its competitiveness relative to commercial adsorbents.

Keywords

Biosorbent, Cocoa Husks, Phosphate, Central Composite Design, Response Surface

1. Introduction

Eutrophication of aquatic environments is currently one of the major environmental challenges worldwide [1] [2]. This phenomenon primarily results from an

excessive enrichment of aquatic ecosystems with nutrients, particularly nitrogen and phosphorus, originating from intensive agricultural activities, industrial effluents, and insufficiently treated domestic wastewater [3]. This nutrient overload promotes excessive proliferation of algae and aquatic plants, leading to a decrease in dissolved oxygen, alteration of biodiversity, degradation of water quality, and significant disturbances to the functioning of aquatic ecosystems [4] [5]. Among the nutrients responsible for this phenomenon, phosphorus is widely recognized as the primary limiting factor of eutrophication in continental waters [6]. In aquatic environments, it occurs in various chemical forms, notably as inorganic phosphates, organic phosphorus compounds, oligophosphates, and polyphosphates [3]. Even at low concentrations, phosphorus is sufficient to stimulate the growth of photosynthetic organisms and accelerate eutrophication: recent studies place the ecological threshold for total phosphorus at around 0.04 $mg{\cdot}L^{-1}$ for surface waters [7]. Under the effect of anthropogenic discharges, this value is nevertheless frequently exceeded in many regions of the world. Moreover, according to [8], a significant proportion of the world's population still depends on untreated surface waters, such as rivers, lakes, and other water bodies, for domestic needs, which reinforces the need to develop water treatment technologies that are effective, economically accessible, and environmentally friendly.

To reduce phosphorus concentrations in effluents, several treatment processes have been developed and widely implemented in wastewater treatment plants. Biological treatments rely on phosphorus assimilation by microorganisms [9] whereas physicochemical routes rely mainly on chemical precipitation with Ca, Fe or Al salts [10] or on coagulation-flocculation using alum [3]. Despite their effectiveness, these techniques present several limitations, notably high operating costs, sometimes complex implementation, substantial consumption of chemical reagents, and the generation of large quantities of secondary sludge requiring further treatment [11]. These drawbacks have encouraged the development of cheaper and greener treatment options.

Among the possible alternatives, adsorption on biosorbents derived from agricultural residues appears as a particularly promising technology. This approach offers numerous advantages, including relatively low cost, abundant availability of raw materials, simple implementation, high efficiency in pollutant removal, and a significant reduction in environmental impact [12] [13]. The use of agricultural waste as adsorbent materials also fits within a circular economy approach, valorizing residual biomass while contributing to the protection of water resources.

Our earlier screening work, based on Plackett-Burma matrix, identified the operating parameters that most strongly govern phosphate uptake [14]. The present paper extends these results by optimizing the way the biosorbent is prepared. A linear (first-order) model derived from a two-level full factorial design (FFD) is tested first, and a central composite design (CCD), which yields a quadratic model, is applied if the linear model proves inadequate. The performance of the developed model is finally compared with results reported in the literature to as-

sess the robustness, reliability, and relevance of the methodological approach adopted.

2. Material and Methods

2.1. Biosorbent Preparation

The cocoa husks, supplied by farmers in the Daloa area (Côte d'Ivoire), were prepared according to the protocol described in our previous work [14]. Briefly, after washing and air-drying at room temperature, the biomass was mechanically ground using a Retsch SK 100 knife mill, then sieved to obtain the desired particle size fractions. The powder was then activated by immersion in a NaOH or H_2SO_4 solution kept under magnetic stirring (350 rpm), at concentrations, durations, and temperatures that varied according to the trial. The activated materials were successively rinsed with tap water and distilled water, then dried before use.

2.2. Investigation of the Optimal Biosorbent Preparation Conditions

Optimization of the biosorbent preparation conditions was carried out using experimental design methodology, a statistical approach that allows the simultaneous study of several parameters and of their interactions within a single series of runs, which the conventional one variable at a time strategy cannot achieve [15]. The phosphate ion removal rate (R, in %) was retained as the single response for evaluating the material's efficiency. A preliminary screening study, carried out using a Plackett-Burman design (PBD), addressed seven preparation variables: biomass nature, particle size, activation time, activation temperature, solid/liquid ratio, type of activating agent, and concentration of the activating solution. Three parameters emerged as significant from this screening and were carried forward to the optimization step: activation temperature (X_1), activation time (X_2), and sodium hydroxide concentration (X_3) [14]. Their experimental domain is given in Table 1. These boundaries were defined based on the screening results, particularly the marked positive effect of the activating agent concentration. These three factors were subsequently studied by means of a full factorial design.

Table 1. Experimental domain of the full factorial design.

Factors	Low level	High level
Temperature (X_1)	40˚C	80˚C
Duration (X_2)	3 h	6 h
Normality (X_3)	0.5 N	2.5 N

The design implemented is thus a duplicated three-factor full factorial design (2^3), corresponding to 16 experimental runs.

The resulting first-degree polynomial model from this design is given by Equation (1).

$$R = a_0 + \sum_{i=1}^{k} a_i x_i + \sum_{ij} a_{ij} x_i x_j \quad (1)$$

Here, a_{ij} denotes the coefficients of the two-factor interactions. Response surface methodology was then applied through a central composite design (CCD) in order to model the removal rate and locate the optimum. A CCD combines three groups of runs: the 2^k points of a two-level factorial design (k being the number of factors), the axial (star) points, and replicated center points. It leads to the second-order polynomial of Equation (2):

$$R = a_0 + \sum a_i X_i + \sum a_{ij} X_i X_j + \sum a_{ii} X_i^2 \quad (2)$$

The a_{ii} coefficients account for the curvature of the response (quadratic effects). Minitab 19 software was used to build the design matrices, estimate the regression coefficients and compute the statistical values for the different experimental designs.

2.3. Methods for Coefficient Evaluation and Model Validation

Each coefficient was tested by multiple linear regression and the overall model by analysis of variance (ANOVA) at the 5% significance level; terms with $p > 0.05$ were discarded. A model was regarded as adequate when its residual sum of squares was lower than one third of the regression sum of squares [16]. The quality of fit was further judged from R^2 and adjusted R^2 [17] and from Fisher's F-test [18]. Predictive accuracy was expressed through the coefficient of variation (CV), defined as:

$$C_V = \frac{1}{n}\left[\sum_{i=1}^{n}\left|\frac{R_{\text{exp}} - R_{\text{cal}}}{R_{\text{exp}}}\right|\right] \times 100 \quad (3)$$

where n is the number of runs, and R_{exp} and R_{cal} are the measured and predicted removal rates, respectively. A CV below 5% was taken as the acceptance criterion [19]. The optimum was located from the contour and three-dimensional response surface plots and then refined with the desirability function of Minitab 19.

2.4. Method for Evaluating the Phosphate Ion Removal Rate

The efficiency of each material was assessed through batch adsorption runs. In each run, 1 g of biosorbent was shaken with 25 mL of a 50 mg/L synthetic phosphate solution in a 100 mL Erlenmeyer flask. The pH was set at 4.7 with 1 N H_2SO_4 or 1 M NaOH, following [3]. The suspensions were stirred magnetically at 300 rpm for 2 h at room temperature and then centrifuged at 4000 rpm for 12 min. The residual phosphate concentration in the supernatant was measured by UV-Visible spectrophotometry at 880 nm, and the removal rate was calculated as follows:

$$R = \frac{C_0 - C_e}{C_0} \times 100 \quad (4)$$

R: phosphate ion removal rate (%)

C_0: initial phosphate ion concentration (mg/L)

C_e: residual phosphate ion concentration (mg/L)

3. Results and Discussion

3.1. First-Degree Model: Full Factorial Design (FFD)

Figure 1 reports the removal rate R (%) obtained for the eight factorial combinations, each run in duplicate.

Removal varied from 66.2% (run 1) to 85.0% (run 8). The lowest response is higher than the lowest one recorded during the screening stage, which indicates that the biosorbent was improved. The mean and median of the responses (76.8% and 79.3%, respectively) are close to each other, which points to a roughly symmetrical distribution of the data [20].

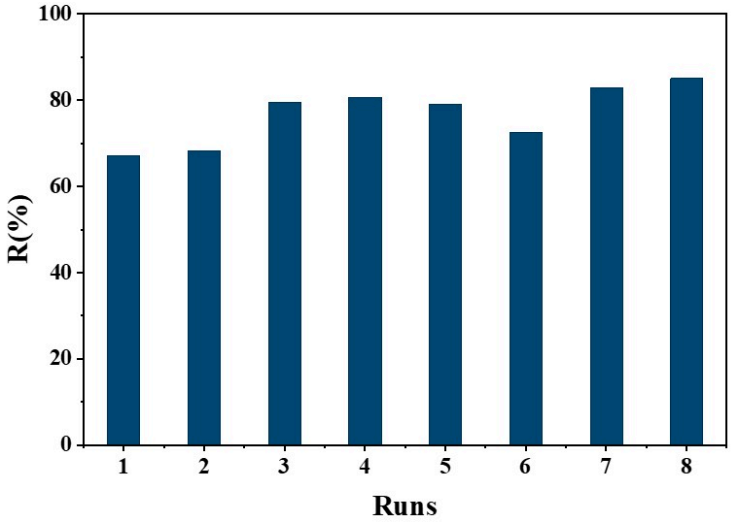


Figure 1. Results of the full factorial design.

Regression of the factorial data in Minitab gave the following linear model, where R_1 is the predicted removal rate:

$$R_1 = 44.2 + 0.134X_1 + 5.63X_2 + 18.5X_3 - 0.019X_1 * X_2 - 0.205X_1 * X_3 - 2.90X_2 * X_3 + 0.036X_1 * X_2 * X_3 \quad (5)$$

The ANOVA of the factorial model is reported in Table 2.

Table 2. Analysis of variance for the full factorial design.

Sources	DF	Adj SS	Adj MS	F-value	p-value
Model	7	632.249	90.321	4.9	0.021
Error	8	150.845	18.856		
Pure error	4	3.411	0.853		
Total	15	783.094			
R^2	80.74%				
R^2_A	63.88%				

With a p-value of 0.021, below the 0.05 threshold, the ANOVA in **Table 2** shows that the linear model is significant as a whole; in other words, the factors studied do affect the removal efficiency [15].

However, closer examination of the other statistical parameters reveals that the linear model cannot be validated, in accordance with the methodological criteria reported by [3] [21]. Indeed, although the model sum of squares is relatively high (632.249), the error sum of squares remains substantial (150.845), reflecting non-negligible dispersion of the residuals [3]. This situation indicates that the model fails to satisfactorily explain the variability observed in the experimental data. Moreover, the presence of a low pure error (3.411) compared to the total error suggests that the observed discrepancy is mainly due to model inadequacy rather than random experimental error [21]. This confirms that the linear structure of the model does not correctly describe the actual behavior of the system studied [11]. Furthermore, the coefficients of determination shown in the table reinforce this conclusion. While R^2 is 80.74%, meaning that about four fifths of the total variability is accounted for by the model, the adjusted R^2 drops to 63.88%, revealing a significant loss of explanatory power once the number of factors and interactions is accounted for [11]. This marked difference between R^2 and adjusted R^2 reflects over-parameterization and insufficient predictive capacity of the model [22]. Thus, despite apparent statistical significance, the first-degree model shows major limitations in terms of adequacy and robustness. In line with recommendations from the literature [23], these results justify rejecting the linear model and highlight the need to resort to a second-order model [3] based on a response surface design, in order to better capture the joint and non-linear effects of the factors. Prior to building this second-order model, the relative weight of each factor and interaction was examined with a pareto chart (**Figure 2**), so as to single out the variables that actually govern removal efficiency.

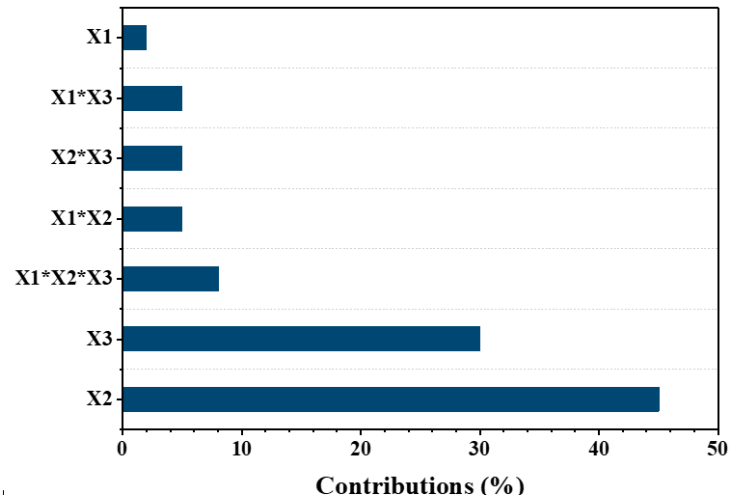


Figure 2. Pareto chart of the standardized effects of the three factors and their interactions.

As can be seen in **Figure 2**, over 80% of the variability in the response is at-

tributable to the activation time (X_2), the sodium hydroxide concentration (X_3), and the interaction between NaOH concentration-activation temperature-duration ($X_1 \cdot X_2 \cdot X_3$). The most influential factor is the activation time (X_2). Next came the normality and the interaction between NaOH concentration-activation temperature-duration ($X_1 \cdot X_2 \cdot X_3$), with respective contributions of 30.0% and 8.0% [11]. The contributions of temperature (X_1), the interaction between activation temperature and activation time ($X_1 \cdot X_2$), and the interaction between activation time and normality ($X_2 \cdot X_3$) each contribute less than 15%. The main effects plot (**Figure 3**) shows the direction and magnitude of the effect of each factor and indicates which level favors phosphate removal.

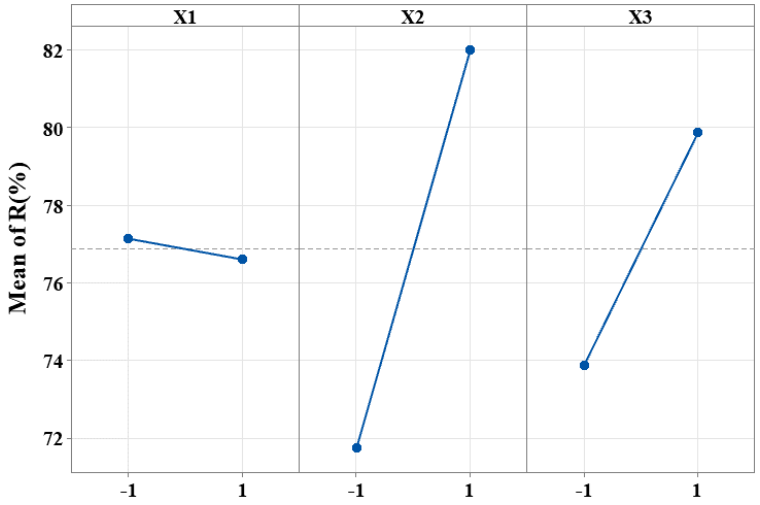


Figure 3. Main effects plot of the factors.

As shown in **Figure 3**, removal efficiency rises with normality (X_3): the mean removal rate goes from about 74% to 80% when the NaOH concentration is raised from 0.5 N to 2.5 N, *i.e.* a gain of about 6 percentage points. Extending the activation time (X_2) from 3 h to 6 h has an even stronger effect, the mean removal rate increasing from about 69% to 82%. Both parameters therefore improve the performance of the biosorbent. A longer and more concentrated alkaline treatment is likely to hydrolyze a larger fraction of lignin and hemicellulose, thereby opening up the porosity and generating oxygen-bearing functional groups that are known to participate in phosphate binding [14]. Similar trends have been reported for activated biosorbents [11] and for activated clays [3]. In contrast, the Pareto chart (**Figure 2**) shows that activation temperature (X_1) has no statistically significant effect, and **Figure 3** even suggests a slight decrease in removal at its high level. Consequently, only activation time and NaOH concentration were kept for the next step. The second-order model used to describe and optimize the response is presented in the following section.

3.2. Central Composite Design (CCD)

The CCD was built with two factors ($k = 2$), namely NaOH concentration (X_1)

and activation time (X_2). It comprised 13 runs distributed as follows:

4 factorial runs (2^2);

4 axial (star) runs ($2k$);

5 replicated runs at the center of the domain.

With $\alpha = (2k)^{1/4} = 1.414$, the coded levels of each factor range from −1.414 to +1.414, which corresponds to 1 - 3 N for NaOH concentration and 4 - 8 h for activation time. The measured responses R_2 (Exp), the values predicted by the model R_2 (Cal) and the corresponding coefficients of variation are listed in Table 3.

Table 3. Matrix, experimental design, removal rate, and coefficients of variation for the central composite design.

Test	Normality	Duration	R_2 (Exp)	R_2 (Cal)	Residual	Cv (%)
1	1.29	4.58	90.08	90.43	−0.35	0.39
2	2.70	4.58	82.34	81.84	0.5	0.6
3	1.29	7.41	93.4	93.11	0.29	0.31
4	2.70	7.41	86.42	85.28	1.14	1.32
5	1	6	95.95	95.69	0.26	0.27
6	3	6	83.14	84.08	−0.94	1.13
7	2	4	83.42	83.29	0.13	0.16
8	2	8	86.79	87.61	−0.82	0.94
9	2	6	83.1	83.27	−0.17	0.2
10	2	6	84.62	83.27	1.35	1.6
11	2	6	82.77	83.27	−0.5	0.6
12	2	6	83.75	83.27	0.48	0.58
13	2	6	82.23	83.27	−1.04	1.26

All CCD runs gave removal rates above 80% (Table 3), which confirms the improvement achieved after the factorial stage. Figure 4 presents the distribution of residuals as a function of fitted values. The residuals appear randomly distributed around zero, with no systematic trend.

No residual exceeds 2 in absolute value, showing close agreement between measured and predicted responses. Fitting the CCD data gave the second-order model of equation (6), in which R_2 is the predicted removal rate:

$$R_2 = 176.8 - 93.3X_1 - 6.03X_2 + 26.47X_1^2 + 0.545X_2^2 + 0.380X_1 * X_2 \quad (6)$$

In this equation, the coefficients express the individual, interaction and quadratic effects of the factors. The ANOVA used to validate the model is summarized in Table 4.

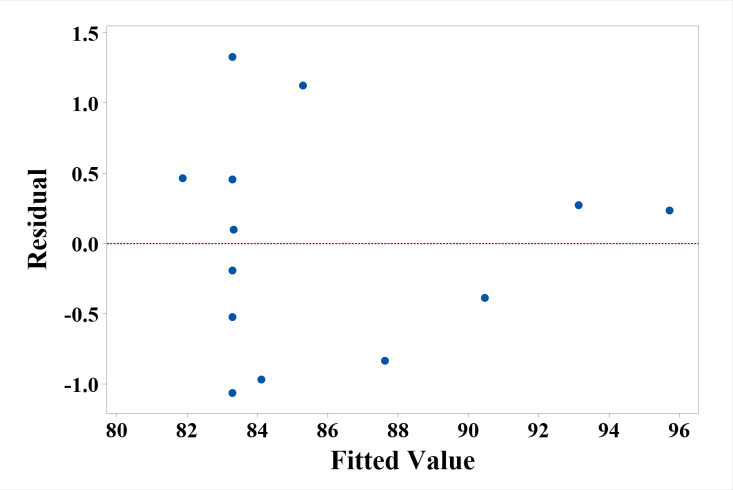


Figure 4. Distribution of residuals versus fitted values.

Table 4. Analysis of variance for the central composite design.

Sources	DF	Adj SS	Adj MS	F-value	p-value
Model	5	232.664	46.533	47.90	0.000
Error	7	6.800	0.971		
Lack-of-fit	3	3.389	1.130	1.33	0.383
Pure error	4	3.411	0.853		
Total	12	239.464			
R^2	97.16%				
R_A^2	95.13%				
CV	0.72%				

In line with the criteria of [24], the residual sum of squares (6.800) is far below the regression sum of squares (232.664), and the model is highly significant ($p < 0.001$). The lack-of-fit test is not significant ($p = 0.383 > 0.05$), so the quadratic form describes the data adequately. Pure error (3.411) represents only 1.42% of the total sum of squares and can therefore be neglected [25]. R^2 (97.16%) and adjusted R^2 (95.13%) are both high and close to each other, which shows good agreement between measured and predicted values and rules out over-fitting. Finally, the mean CV (0.72%) is well below the 5% limit. Together, these results validate the proposed quadratic model [24]-[26].

3.3. Optimization of the Phosphate Ion Removal Rate

The optimum was first sought graphically from the contour plot in **Figure 5**, which shows that removal rates above 95% can be achieved without leaving the experimental domain. The optimal region corresponds to combinations of NaOH concentration (X_1) and activation time (X_2) that place the response on or beyond

the 99% contour (darkest blue zone). The problem therefore consists in finding the coded values of X_1 and X_2, within the design limits, that maximize R_2 as described by the second-degree polynomial.

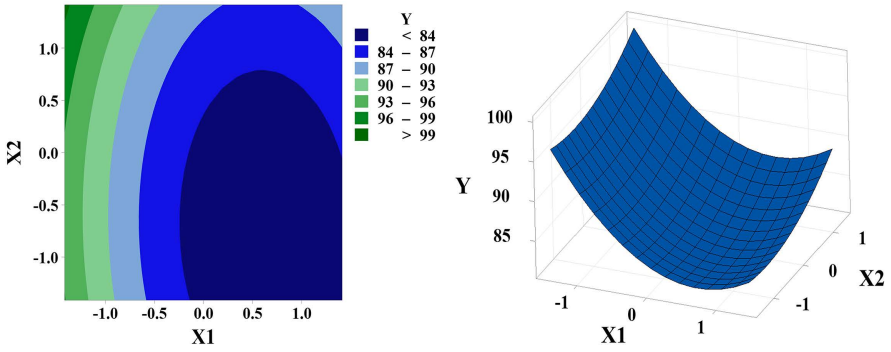


Figure 5. Contour and response surface plots.

These coded values were then calculated with the desirability function of Minitab (Figure 6), the target being the maximum phosphate removal rate.

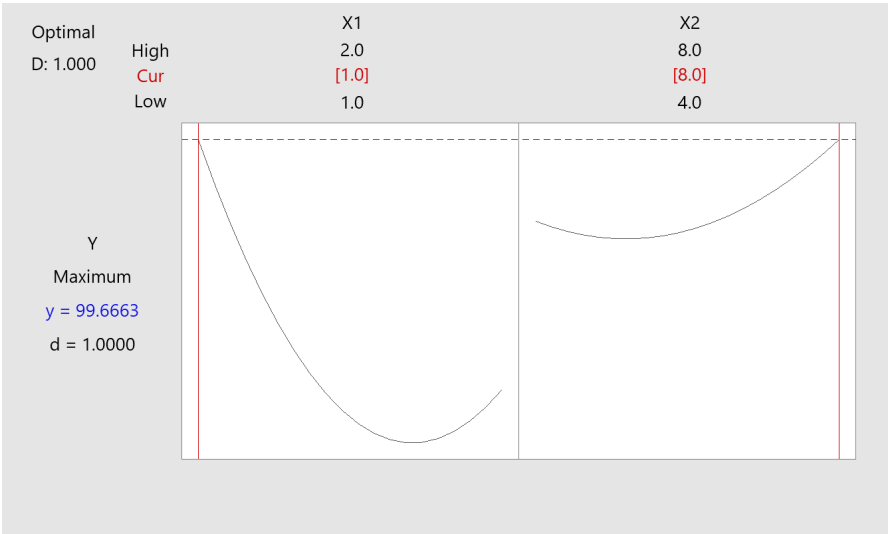


Figure 6. Desirability function.

According to Figure 6, a desirability of 1 is reached for a predicted removal rate of 99.67%. This optimum lies at −1.414 for NaOH concentration and +1.414 for activation time in coded units, which, after conversion to real units, gives 1 N NaOH and 8 h of activation. The 95% confidence interval of this prediction ranges from 94% to 100% (Table 5). Since the optimum lies at the boundary of the experimental domain, slightly better conditions outside the studied range cannot be excluded. Three additional (control) runs were performed under these conditions.

3.4. Control Test Results

Table 6 gives the results of the confirmation runs.

Table 5. Response prediction.

Factors	Settings
Normality	1 N
Duration	8 h
Response	Fitted value 99.67%
Removal percentage	95% CI (94 - 100)

Table 6. Control test results under optimal biosorbent preparation conditions.

Test	NaOH Concentration	Duration (*H*)	R_2 cal (%)	R_2 exp (%)	Mean removal rate (%)
1	1	8	99.67	97.2	
2	1	8	99.67	98.8	98.23
3	1	8	99.67	98.7	

The three control tests gave a mean removal rate of 98.23% (standard deviation 0.90). The difference from the predicted value (99.67%) is 1.44 percentage points, well within the 5% tolerance, which validates the model. This level of performance agrees with recent biosorption studies: comparable removal efficiencies, for various pollutants, have been reported for biosorbents prepared from Saba senegalensis hulls [11], argan shells [27], green walnut hulls [28], cocoa pod husks [29] and waste perlite [30], and they are of the same order as those of activated carbons [31] [32]. This high efficiency results both from the statistical optimization of the preparation conditions [21] [33] [34] and from the NaOH activation step, which enhanced the adsorption capacity of the material.

4. Conclusion

This work optimized the preparation of a cocoa husk biosorbent for phosphate removal using design-of-experiments tools. Following a preliminary screening, three variables were examined: activation temperature, activation time and NaOH concentration. The full factorial design showed that temperature had no significant effect, whereas activation time and NaOH concentration were the dominant factors. These two variables were then optimized by combining a central composite design, response surface analysis and the desirability function of Minitab 19. The best results were obtained with 1 N NaOH for 8 h, which gave a mean removal rate of 98.23%, close to the 99.67% predicted by the model and thus confirming the reliability of the approach. Cocoa husks therefore represent a low-cost and sustainable biosorbent for phosphorus removal, with an efficiency comparable to that of activated carbons, while turning an agro-industrial residue into a useful material in line with circular economy principles. Further work is still needed to assess the industrial feasibility of the process, including a techno-economic analysis. A detailed characterization of the material (FTIR, SEM, BET, pHPZC) will

also be required to identify the functional groups involved, its morphology and textural properties, and the adsorption mechanisms before any scale-up.

Acknowledgements

We thank the management of the Laboratoire des Sciences et Technologies de l'Environnement, Université Jean Lorougnon Guédé (Daloa, Côte d'Ivoire), for providing laboratory facilities and for their support during this study.

Author Contributions

Christian Landry Yapi: Conceptualization, Methodology, Investigation, Formal analysis, Data curation, Visualization, Writing-original draft. Yapo Hermann Aristide Yapi: Methodology, Validation, Writing-review & editing. David Léonce Kouadio: Formal analysis, Validation, Writing-review & editing. Kouassi Serge Gbamélé: Investigation, Resources, Writing-review & editing. Issifou Ouattara Mama: Methodology, Validation, Writing-review & editing. Brou Dibi: Conceptualization, Supervision, Project administration Writing-review & editing. All authors have read and agreed to the published version of the manuscript.

Conflicts of Interest

The authors declare no conflicts of interest regarding the publication of this paper.

References

[1] Ano, J., Henri Briton, B.G., Kouassi, K.E. and Adouby, K. (2020) Nitrate Removal by Electrocoagulation Process Using Experimental Design Methodology: A Techno-Economic Optimization. *Journal of Environmental Chemical Engineering*, **8**, Article 104292. https://doi.org/10.1016/j.jece.2020.104292

[2] Eltelib, H.A., Muna, A.H. and Eltom E.A. (2006) The Effect of Nitrogen and Phosphorus Fertilization on Growth, Yield and Quality of Forage Maize (*Zea mays* L.). *Journal of Agronomy*, **5**, 515-518. https://doi.org/10.3923/ja.2006.515.518

[3] Adjoumani, Y.J., Dablé, P.J.M.R., Kouassi, K.E., Gueu, S., Assémian, A.S. and Yao, K.B. (2019) Modeling and Optimization of Two Clays Acidic Activation for Phosphate Ions Removal in Aqueous Solution by Response Surface Methodology. *Journal of Water Resource and Protection*, **11**, 200-216. https://doi.org/10.4236/jwarp.2019.112012

[4] Downing, J.A. (2014) Limnology and Oceanography: Two Estranged Twins Reuniting by Global Change. *Inland Waters*, **4**, 215-232. https://doi.org/10.5268/iw-4.2.753

[5] Smith, V.H. and Schindler, D.W. (2009) Eutrophication Science: Where Do We Go from Here? *Trends in Ecology & Evolution*, **24**, 201-207. https://doi.org/10.1016/j.tree.2008.11.009

[6] Schindler, D.W., Hecky, R.E., Findlay, D.L., Stainton, M.P., Parker, B.R., Paterson, M.J., *et al*. (2008) Eutrophication of Lakes Cannot Be Controlled by Reducing Nitrogen Input: Results of a 37-Year Whole-Ecosystem Experiment. *Proceedings of the National Academy of Sciences*, **105**, 11254-11258. https://doi.org/10.1073/pnas.0805108105

[7] Wu, F., Fang, Y., Feng, M., Xie, Z., Zhu, L. and Feng, J. (2022) Developing Ecological

Thresholds for Nitrogen and Phosphorus in the Haihe River Basin in China. *International Journal of Environmental Research and Public Health*, **19**, Article 16951. https://doi.org/10.3390/ijerph192416951

[8] UN-WATER (2017) Rapport mondial des Nations Unies sur la mise en valeur des ressources en eau 2017: Les eaux usées: une ressource inexploitée. UNESCO. https://unesdoc.unesco.org/ark:/48223/pf0000247551

[9] Rejsek, F. (2002) Analyse des eaux: Aspects réglementaires et techniques. Centre Régional de Documentation Pédagogique (CRDP) d'Aquitaine, 360 p.

[10] Zran, E., Yao, B., Trokourey, A., Yobouet, A. and Drogui, P. (2015) An Optimized Pathway for Phosphate Ions Removal from Aqueous Solution Based on Experimental Design Methodology. *International Journal of Environmental Science and Technology*, **12**, 3117-3124. https://doi.org/10.1007/s13762-014-0738-1

[11] Gouledehi, S.G., Kouadio, D.L., Dalogo, K.A.P., Yapi, Y.H.A., Akéssé, D.P.V. and Dibi, B. (2025) Optimisation of the Process for Converting Saba Senegalensis Hulls into Biosorbents. *Journal of Materials and Environmental Science*, **16**, 354-370.

[12] Enache, A.C., Cojocaru, C., Samoila, P., Ciornea, V., Apolzan, R., Predeanu, G., *et al*. (2023) Adsorption of Brilliant Green Dye onto a Mercerized Biosorbent: Kinetic, Thermodynamic, and Molecular Docking Studies. *Molecules*, **28**, Article 4129. https://doi.org/10.3390/molecules28104129

[13] Mansour, R., Simeda, M.G. and Zaatout, A. (2020) Adsorption Studies on Brilliant Green Dye in Aqueous Solutions Using Activated Carbon Derived from Guava Seeds by Chemical Activation with Phosphoric Acid. *Desalination and Water Treatment*, **202**, 396-409. https://doi.org/10.5004/dwt.2020.26147

[14] Yapi, C.L., Yapi, Y.H.A., Mama, I.O. and Kouadio, D.L. (2026) Removal of Nutrient Salts: Comparative Study of Biosorbents Derived from Cocoa and Rubber Agricultural Wastes. *Asian Journal of Science and Technology*, **17**, 14338-14342.

[15] Tinsson, W. (2010) La Notion de Plan d'expérience. In: *Mathématiques et Applications*, Springer, 3-37. https://doi.org/10.1007/978-3-642-11472-4_1

[16] Bezerra, M.A., Ferreira, S.L.C., Novaes, C.G., dos Santos, A.M.P., Valasques, G.S., da Mata Cerqueira, U.M.F., *et al*. (2019) Simultaneous Optimization of Multiple Responses and Its Application in Analytical Chemistry—A Review. *Talanta*, **194**, 941-959. https://doi.org/10.1016/j.talanta.2018.10.088

[17] Baudot, J.Y. (2018) Le coefficient de détermination. http://www.jybaudot.fr/Correl_regress/coeffdeterm.html

[18] Maataoui, Y.E., Alehyen, S., Fadil, M., Aouan, B., Liba, A., Saufi, H., *et al*. (2025) Application of Central Composite Design for Optimizing Mechanical Performance of Geopolymer Paste from Fly Ash Using the Mechanosynthesis Method: Structural and Microstructural Analysis. *Iranian Journal of Science and Technology, Transactions of Civil Engineering*, **49**, 2481-2501. https://doi.org/10.1007/s40996-024-01601-8

[19] Ncibi, M.C., Mahjoub, B. and Seffen, M. (2008) Étude de la Biosorption du Chrome (VI) Par Une Biomasse Méditerranéenne: *Posidonia oceanica* (L.) Delile. *Revue des sciences de l'eau*, **21**, 441-449. https://doi.org/10.7202/019166ar

[20] Mahunon, S.E.R., Akowanou, A.V.O., Aina, M.P., Yao, B.K. and Sohounhloué, D.K.C. (2015) Elimination of Carbon, Nitrogen and Phosphorus in Domestic Wastewater through a Series of Anaerobic and Aerobic Reactors for a Developing Country Like Benin. *American Journal of Analytical Chemistry*, **6**, 577-584. https://doi.org/10.4236/ajac.2015.67056

[21] Omwoyo, F.O. and Otieno, G. (2024) Optimization of Methylene Blue Dye Adsorp-

tion onto Coconut Husk Cellulose Using Response Surface Methodology: Adsorption Kinetics, Isotherms and Reusability Studies. *Journal of Materials Science and Chemical Engineering*, **12**, 1-18. https://doi.org/10.4236/msce.2024.122001

[22] Lambert, A., Drogui, P., Daghrir, R., Zaviska, F. and Benzaazoua, M. (2014) Removal of Copper in Leachate from Mining Residues Using Electrochemical Technology. *Journal of Environmental Management*, **133**, 78-85. https://doi.org/10.1016/j.jenvman.2013.11.036

[23] Rittisak, S., Dechewa, P., Savedboworn, W. and Phungamngoen, C. (2023) Application of the Plackett-Burman Design for Screening and Optimisation of Factors Affecting the Aqueous Extract for Total Anthocyanin Content of Broken Riceberry Rice. *International Food Research Journal*, **30**, 649-655. https://doi.org/10.47836/ifrj.30.3.09

[24] Oelofse, M., Rack, R., Hilden, M. and Langguth, P. (2024) Optimization of Product Characteristics of Porous Carbon Agglomerates Using a Design of Experiments in Fluidized Bed Agglomeration. *Particuology*, **89**, 258-269. https://doi.org/10.1016/j.partic.2023.10.017

[25] Suditu, G.D., Blaga, A.C., Tataru-Farmus, R., Zaharia, C. and Suteu, D. (2022) Statistical Analysis and Optimization of the Brilliant Red HE-3B Dye Biosorption onto a Biosorbent Based on Residual Biomass. *Materials*, **15**, Article 7180. https://doi.org/10.3390/ma15207180

[26] Archbold, T. and Carson, J.K. (2023) Optimisation of a Grass Cutting Blade Using Design of Experiments with Qualitative and Quantitative Performance Metrics. *Biosystems Engineering*, **234**, 66-80. https://doi.org/10.1016/j.biosystemseng.2023.08.013

[27] Ifguis, O., Ziat, Y., Ammou, F., Bouhdadi, R., Mbarki, M. and Benchagra, M. (2022) Theorithecal and Experimental Study on the Thermodynamic Parameters and Adsorption of Methylene Blue on "Argania Shells" in Industrial Waters. *South African Journal of Chemical Engineering*, **41**, 211-222. https://doi.org/10.1016/j.sajce.2022.06.010

[28] Coşkun, Y.İ. (2022) Investigation of Adsorption Performances of Green Walnut Hulls for the Removal of Methylene Blue. *Desalination and Water Treatment*, **247**, 281-293. https://doi.org/10.5004/dwt.2022.28075

[29] Léonce, K.D., Aristide, Y.Y.H., Jules-César, M.D.E., *et al*. (2023) Contribution to the Modeling of a Biosorbent Derived from Cocoa Pod Shells on the Methylene Blue Index. *The American Journal of Applied Chemistry*, **11**, 50-59.

[30] Selengil, U. and Yıldız, D. (2022) Investigation of the Methylene Blue Adsorption onto Waste Perlite. *Desalination and Water Treatment*, **262**, 235-247. https://doi.org/10.5004/dwt.2022.28530

[31] Kamdod, A.S. and Pavan Kumar, M.V. (2022) Adsorption of Methylene Blue and Methyl Orange on Tamarind Seed Activated Carbon and Its Composite with Chitosan: Equilibrium and Kinetic Studies. *Desalination and Water Treatment*, **252**, 408-419. https://doi.org/10.5004/dwt.2022.28270

[32] Lee, H., Fiore, S. and Berruti, F. (2023) Adsorption of Methyl Orange and Methylene Blue on Activated Biocarbon Derived from Birchwood Pellets. *Biomass and Bioenergy*, **191**, Article 107446. https://doi.org/10.1016/j.biombioe.2024.107446

[33] Kebir, M., Benramdhan, I., Nasrallah, N., Tahraoui, H., Bait, N., Benaissa, H., *et al*. (2023) Surface Response Modeling of Homogeneous Photo Fenton Fe(III) and Fe(II) Complex for Sunlight Degradation and Mineralization of Food Dye. *Catalysis Communications*, **183**, Article 106780. https://doi.org/10.1016/j.catcom.2023.106780

[34] Meledje, D.E.J.C., Yapi, Y.H.A., Kouadio, D.L., Akesse, D.P.V. and Yeo, K. (2024) Optimized Adsorption of Small and Medium Molecules by a Biosorbent Based on Hevea Hulls. *Journal of Materials Science and Chemical Engineering*, **12**, 69-83. https://doi.org/10.4236/msce.2024.129004